Bioorganic & Medicinal Chemistry 21 (2013) 703–711

Contents lists available at SciVerse ScienceDirect

Bioorganic & Medicinal Chemistry

journal homepage: www.elsevier.com/locate/bmc

SiO_2 nanoparticles as platform for delivery of nucleoside triphosphate analogues into cells

Svetlana V. Vasilyeva [a,*], Vladimir N. Silnikov [a], Natalia V. Shatskaya [b], Asya S. Levina [a], Marina N. Repkova [a], Valentina F. Zarytova [a]

[a] Institute of Chemical Biology and Fundamental Medicine, Lavrent'ev Ave., 8, Novosibirsk 630090, Russia
[b] Institute of Cytology and Genetics, Lavrent'ev Ave., 10, Novosibirsk 630090, Russia

ARTICLE INFO

Article history:
Received 7 September 2012
Revised 20 November 2012
Accepted 24 November 2012
Available online 11 December 2012

Keywords:
SiO_2 nanoparticles
Nucleoside triphosphates
'Click' chemistry
Delivery into cells
Substrate properties

ABSTRACT

A system for delivery of analogues of 2′-deoxyribonucleoside triphosphate (dNTP) based on SiO_2 nanoparticles was proposed. A simple and versatile method was developed for the preparation of SiO_2–dNTP conjugates using the 'click'-reaction between premodified nanoparticles containing the azido groups and dNTP containing the alkyne-modified γ-phosphate group. The substrate properties of SiO_2–dNTP were tested using Klenow fragment and HIV reverse transcriptase. Nucleoside triphosphates being a part of the SiO_2–dNTP nanocomposites were shown to be incorporated into the growing DNA chain. The rate of polymerization with the use of SiO_2–dNTP or common dNTP in case of HIV reverse transcriptase differed insignificantly. It was shown by confocal microscopy that the proposed SiO_2–dNTP nanocomposites bearing the fluorescent label penetrate into cells and even into cellular nuclei.

1. Introduction

Abnormal nucleosides are known to be used as etiotropic antiviral preparations.[1,2] However, the active antiviral form is not nucleoside analogues themselves but their 5′-triphosphates, which are major substrates for DNA and RNA viral polymerases. The main reason of using high doses of nucleoside analogues as antiviral preparations is a low level of their intracellular accumulation, the necessity of their intracellular phosphorylation, drug metabolism and deactivation, and rapid clearance from the bloodstream. Moreover, the phosphorylation of nucleoside analogues with cellular enzymes to form corresponding 5′-triphosphates is much less efficient as compared to natural nucleosides. This also leads to the use of high concentrations of nucleoside substrate, and thus to an increase in toxicity.

This problem could be solved by using phosphorylated forms of nucleoside analogues: mono- or, better, triphosphates. Unfortunately, it is well known that nucleoside triphosphates are hardly internalized by cells when applied alone. Therefore, the search for efficient vehicles for nucleoside triphosphates remains an urgent problem.

There are different approaches to create the delivery systems for nucleoside triphosphates. One of the first systems to deliver nucleoside analogues into cells were liposomes.[3] Liposomes could be considered as an ideal system for delivering drugs, but their use is limited because of serious drawbacks, namely: the high instability and time consuming preparation.[4] The polymeric drug delivery system for analogues of nucleoside triphosphates was proposed in the work of Vinogradov et al.[5] A noncovalent complex of the nucleoside 5′-triphosphate analogue with polyethyleneimine was created and placed in the nanogel (polymer consisting of polyethylene glycol and polyethylenimine). The delivery of nucleoside triphosphates analogues with this system was shown to be quite high; however, the nanocomposite appeared to be more toxic by two orders of magnitude than the non-phosphorylated nucleoside analogue. The cytotoxicity of the delivery system is related to its cationic nature[6,7] with its ability to damage membranes[8,9] and bind important cellular components.[10]

The only known successful applications of dNTPs are covalent phospholipide conjugates of anti-HIV drug, 3′-azidothymidine (AZT), which demonstrate a higher bioavailability and a lower toxicity than AZT of itself.[11]

To address the problem of drug transportation into cells, nanobiotechnology is quite actively involved. The integration of biological and nonbiological materials resulting in functional devices is an interdisciplinary multiscale task of great practical importance.[12] A variety of nanomaterials are recently proposed as vehicles for drug delivery.[13] The main important requirements for such materials are the ability to penetrate into eukaryotic cells, low toxicity, biocompatibility, biodegradation, etc. Nanoparticles of titanium dioxide and silicon dioxide are attracted special attention due to

* Corresponding author. Tel.: +7 383 3635183; fax: +7 383 3635182.
E-mail address: svetlana2001@gmail.com (S.V. Vasilyeva).

0968-0896/$ - see front matter © 2012 Elsevier Ltd. All rights reserved.
http://dx.doi.org/10.1016/j.bmc.2012.11.057

their biocompatibility, stability and the possibility of modifying the surface for the immobilization of various compounds.[14,15]

The effectiveness of penetration of nanoparticles depends on their size and the cell type. It was shown that SiO_2 nanoparticles of 40–70 nm in size penetrate into the Hep-2 and Caco-2 cells cells and in their nuclei.[16,17] Some experiments demonstrated the ability of SiO_2 nanoparticles to biodegradation.[15,18]

The goal of this work was to design nanocomposites consisting of analogues of 2′-deoxyribo nucleoside triphosphates (dNTP) immobilized onto SiO_2 nanoparticles and to study their substrate properties in reactions catalyzed by DNA polymerases and their ability to penetrate into eukaryotic cells.

2. Results and discussion

To use SiO_2 nanoparticles as platform for delivery of dNTP analogues into cells we suggested a simple and versatile method of their covalent attachment to nanoparticles: the 'click'-reaction between premodified nanoparticles containing the azido groups and dNTP containing the alkyne-modified gamma-phosphate group.

Among various carbon–heteroatom bond formation reactions, the copper catalyzed Huisgen 1,3-dipolar cycloaddition is the premier example of click chemistry known for its high degree of selectivity and stability.[19] Moreover, the resulting triazole ring itself has been shown to possess a variety of biological functions including anti-HIV, antibacterial, and potent antihistamine activity.[20–22] We took advantage of this click chemistry to develop the drug delivery system. Scheme 1 illustrates the copper(I)-catalyzed azide–alkyne cycloaddition (CuAAC) reaction between premodified nanoparticles containing the azide groups (**1**) and nucleoside triphosphates containing the alkyne-modified γ-phosphate (**2** or **3**) that resulted in the formation of the desired nanocomposites (**4** or **5**).

Introduction of the alkyne group into the γ-phosphate of dNTP was performed using the 3-aminopropoxypropynyl linker (**L**, Schemes 2 and 3).[23] Activation of the terminal phosphate group was achieved in the presence of the nucleophilic catalyst.[24] Despite the facts that this reaction is not universal, depends on the nature of conjugating components, and sometimes is accompanied by a large number of side products, the yields of the desired products were satisfactory (52% for (**2**) and 64% for (**3a**), Schemes 2 and 3).

To study the penetration of the proposed nanocomposites into cells, we synthesized fluorescent-labeled $dUTP^{Flu}$ (**3**) by the introduction of the fluorescein residue in compound **3a**. The *N*-(3-propynyloxypropyl trifluoroacetamide linker group[23] was attached to the C5 position of 2′-deoxyuridine followed by the deprotection of the amino group and introduction of the fluorescein residue (Scheme 3). Target 5-{3-[3-(fluorescein-5-yl-thioureido)propoxy] prop-1-ynyl}-2′-deoxyuridine-5′-{*N*-[3-(prop-1-ynyl)oxypropyl]-gamma-amino}-triphosphate **3** was obtained from **3a** with a yield of 70%. The structures of the final products **2, 3** were confirmed by ^1H and ^{31}P NMR and mass spectrometry (MS).

Nanoparticles containing the azide groups (**1**) were prepared by the treatment of SiO_2–NH_2 nanoparticles with N-hydroxysuccinimide ester of azidohexanoic acid (*N*-SEHA) (**1b**, Scheme 4A), which was synthesized according to Scheme 4B. Compound **1** has the characteristic azide absorption band in the IR spectra in contrast to the unmodified nanoparticles. (IR spectra of SiO_2–NH_2 (IR SiO_2–NH_2) and product **1** (IR **1**) see in Supplementary data). The azido group band of azidohexanoic acid (AHA) of a high intensity is observed in the range of 2286.75–1998.78 cm^{-1}. An approximately 10-fold excess of *N*-SEHA over the amino groups in SiO_2–NH_2 was shown to be sufficient for the successful conversion of the amino groups into the azido groups (Table 1, IR AHA, IR Samples **1**–**3** in Supplementary data). The evaluation of the amount of the amino groups with picric acid[25] before and after the reaction showed that ~85% of the amino groups were modified. Not all amino groups in SiO_2–NH_2 are, probably, accessible for the reaction due to steric hindrances that results in the non-quantitative yield of the reaction. The capacity of the prepared azido modified nanoparticles for the azido groups was evaluated to be 0.43 μmol/mg.

The yield of the 'click'-reaction between the azido-modified nanoparticles and alkyne-containing compounds was evaluated by the disappearance of the signal of the azido group in the IR spectrum. The reaction between the azido-modified nanoparticles **1** and the 3-aminopropoxypropynyl linker group (**L**) was carried out as the control experiment (**6**, Scheme 4C). The IR spectrum of product **6** showed the absence of the azido group signal (compare IR **6** and IR **1** in Supplementary data) that confirmed the formation of the covalent bond between the linker and the nanoparticles. A partial disappearance of the azido group band was shown when the azido-nanoparticles were treated by alkyne-modified γ-phosphate **2** or **3** under the 'click' reaction condition (IR **1** and **4**, IR **1** and **5** in Supplementary data). Usually, the yield in the azide–alkyne Huisgen's cycloaddition reaction for small molecules exceeds 80%;[26–28] however, the kinetics of this reaction for small and large

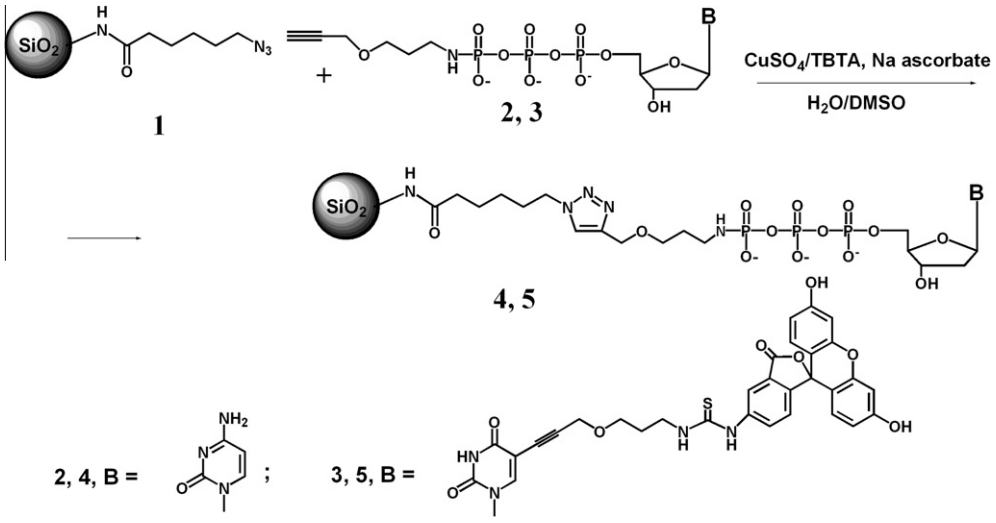

Scheme 1. Synthesis of nanocomposites SiO_2–dCTP and SiO_2–$dUTP^{Flu}$ via the copper(I)-catalyzed azide–alkyne cycloaddition (CuAAC) reaction between the premodified nanoparticles containing the azide groups and nucleoside triphosphates containing the alkyne-modified gamma-phosphate.

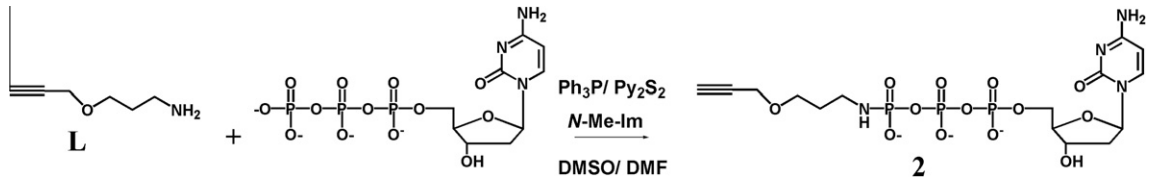

Scheme 2. Synthesis of the alkyne-modified dCTP—2′-deoxycytidine-5′-{*N*-[3-(prop-1-ynyl)oxypropyl]-gamma-amino}-triphosphate. Yield 52%.

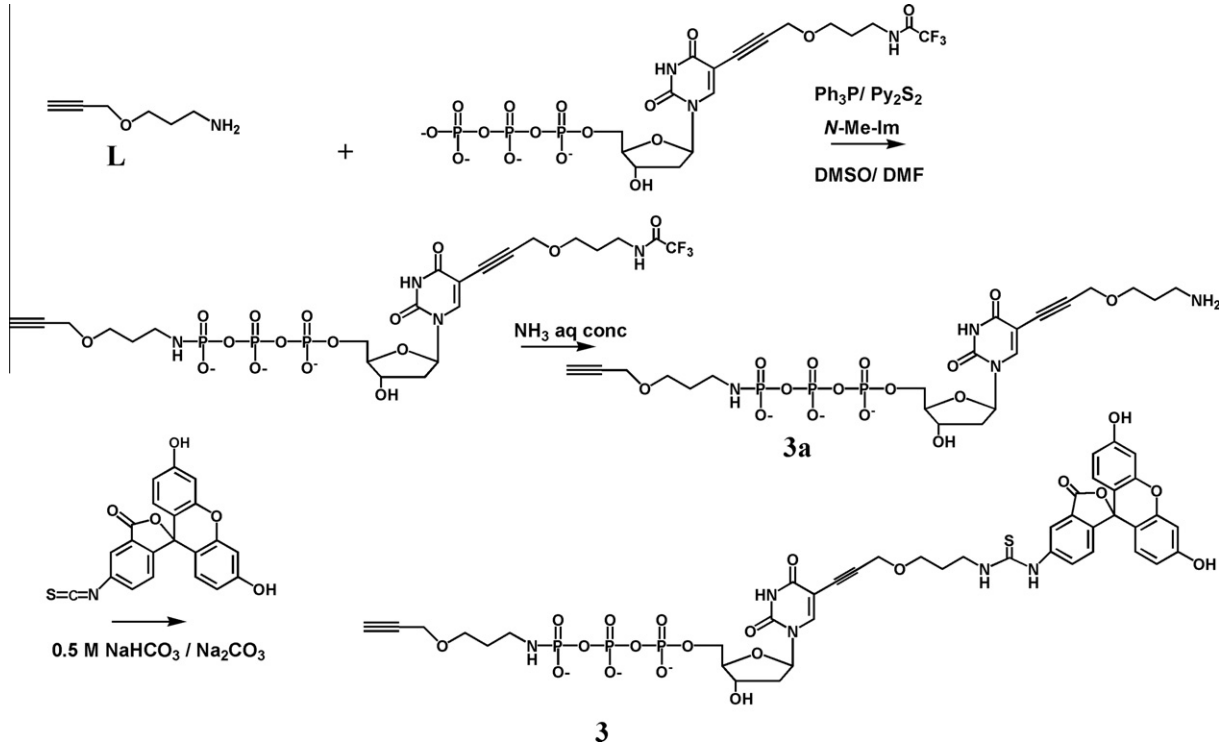

Scheme 3. Synthesis of alkyne-modified dUTP^{Flu} bearing the fluorescent label—5-{3-[3-(fluorescein-5-yl-thioureido)propoxy]prop-1-ynyl}-2′-deoxyuridine-5′-{*N*-[3-(prop-1-ynyl)oxypropyl]-gamma-amino}-triphosphate. Overall yield 45%.

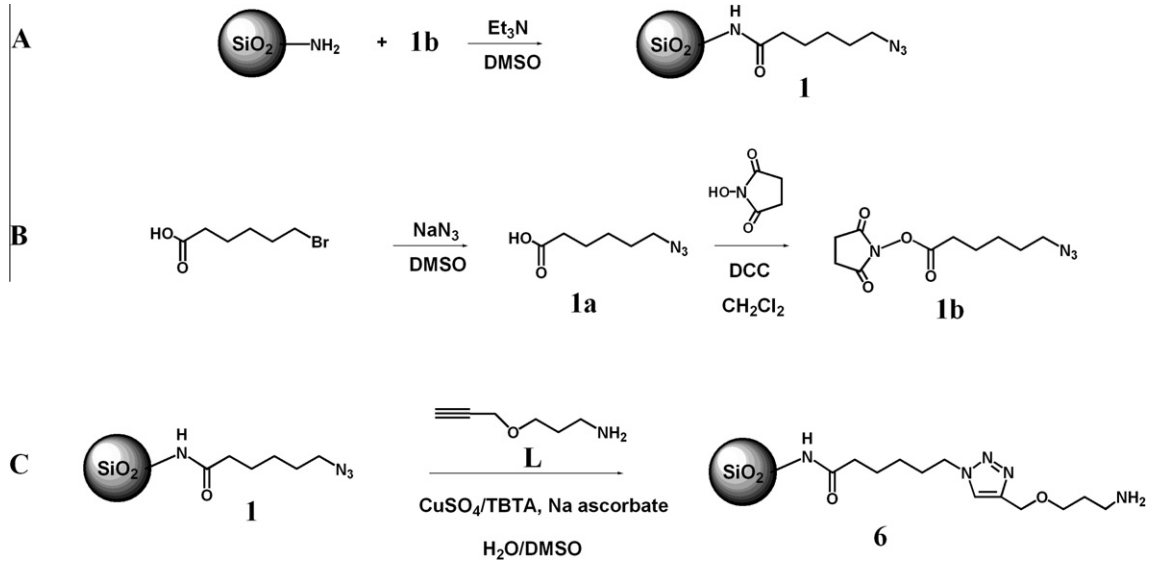

Scheme 4. (A) Synthesis of the azidomodified SiO_2 nanoparticles. Overall yield 63%. (B) Synthesis of the *N*-hydroxysuccinimide ester of 6-azidohexanoic acid (*N*-SEHA). (C) Synthesis of the SiO_2–L–NH_2 by 'click'-reaction. Yield approximately100%.

molecules significantly differs from each other. As reported, the yield of this reaction is reduced below 50% when two polymers are involved in the cycloaddition reaction.[29] The yield is expected to decrease even more when the accessibility of the azido groups on solid particles is limited due to steric hindrances. The yield of the attachment of triphosphate **2** to nanoparticles evaluated by measuring the optical density of the resulting product SiO_2–dCTP dissolved in 0.2 M NaOH was 58%. The capacity of SiO_2–dCTP for the triphosphate was evaluated to be 0.25 μmol/mg. Altogether, these data confirmed the successfulness of the Huisgen's 1,3-dipolar cycloaddition reaction for the preparation of the SiO_2–dNTP nanocomposites.

It was shown by the Small-Angle X-ray Scattering (SAXS) method[30,31] that the size of the initial SiO_2–NH_2 nanoparticles (up to 22–24 nm) insignificantly differed from that of the final SiO_2–dNTP nanoparticles (up to 25–27 nm), that is the difference was not more than 2–3 nm (see diagrams of the particles size distribution in Supplementary data). This is a reasonable result considering that the size of dNTP with the linker (4–5 nm) is much lower than the size of one nanoparticle and that this molecule can be not necessarily positioned perpendicular to the surface of the particle.

The prepared nanocomposites were studied for their ability to be substrates for DNA polymerases. The property of the synthesized SiO_2–dCTP along with other native dNTPs to be involved in the growing DNA chain was tested on a model system consisting of a 30-mer DNA template, 16-mer DNA primer. Klenow fragment (DNA polymerase I from *Escherichia coli*) and HIV reverse transcriptase were used as DNA polymerases.

5'-d(TCTGCTGTACATGGCACATGGAATTGATTA) template (30-mer)
3'-d(TACCGTGTACCTTAAC)p[^{32}P] primer (16-mer)

Figure 1 demonstrates the results of polymerization in the system with Klenow fragment. The use of all four native triphosphates led to the formation of the full length 26-mer oligonucleotides (Fig. 1, lane 1). When only three native triphosphates of guanosine, adenosine, and thymidine were used, the chain of the synthesized DNA fragment was limited by a truncated 19-mer fragment according to the template-primer structure (Fig. 1, lane 2). The replacement of dCTP by SiO_2–dCTP in the mixture of triphosphates provided the polymerization similar to the use of four natural triphosphates, although some amount of the 19-mer fragment was still observed (compare lanes 3 and 1 in Fig. 1). The use of supernatant from the SiO_2–dCTP suspension led to the formation of the 19-mer as it was in the absence of dCTP (compare lanes 4 and 2 in Fig. 1). This means that all dCTP in the SiO_2–dCTP nanocomposite is strongly associated with nanoparticles and does not go into solution.

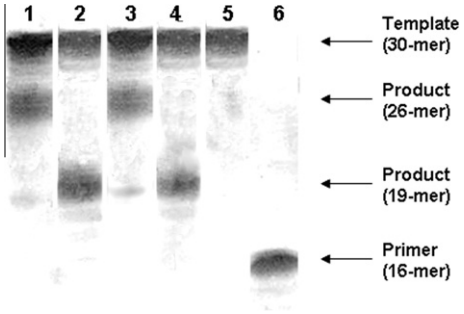

Figure 1. Electrophoresis in 20% PAAG of the extension products in the template (30-mer)/primer (16-mer) system in the presence of Klenow fragment (1×10^{-3} U) and four dNTPs (lane 1), three native dNTP except dCTP (lane 2), three native dNTP + SiO_2–dCTP (lane 3), three native dNTP + supernatant from SiO_2–dCTP suspension (lane 4), template (lane 5), primer (lane 6). 10^{-6} M for the template, 1×10^{-6} M for the primer, 1×10^{-5} M for dNTPs; SiO_2– dCTP —0.07 mg/ml (1×10^{-5} M for triphosphate) reaction time 60 min, 37 °C. Spots were visualized with Stains All.

Then we compared the kinetics of polymerization in the reaction mixtures containing four native dNTPs or three native dNTPs and SiO_2–dCTP instead of dCTP. Both polymerases were used in these experiments (Figs. 2 and 3). Concentrations of dCTP in the nanocomposite and each of the native triphosphates were the same. It is seen from the kinetic curves that the reaction rate is slightly lower in the case of using SiO_2–dCTP instead of dCTP although the initial primer disappears in 1–1.5 h in all cases. As can be expected, the use of SiO_2–dCTP instead of dCTP leads to some retardation of the reaction at the steps of the formation of 19-mer and 23-mer, that is immediately before the involvement of SiO_2–dCTP in the reaction. This is particularly clearly seen from Figure 2B at the initial reaction stages. Interestingly, that in the case of Klenow fragment, the initial reaction rate when using SiO_2–dCTP instead of dCTP significantly differs from that when using four native triphosphates (Fig. 2), while in the case of RT HIV (virus polymerase), this difference is not so pronounced (Fig. 3). It offers hope that the proposed nanocomposites will be better recognized by virus DNA polymerases than cellular DNA polymerases.

Thus, the results show the availability of the SiO_2–dNTP as a substrate for DNA polymerases.

The next step of our investigation was to show whether the proposed nanocomposites can penetrate into cells. The SiO_2–$dUTP^{Flu}$ nanocomposite **5** bearing the fluorescent label at the 5 position of 2′-deoxyuridine was synthesized for this purpose. Figure 4 demonstrates the image of HeLa cells after incubation with this nanocomposite. It is seen that the fluorescent label is uniformly distributed within the cells. It should be noted that the nanocomposite penetrates not only into the cellular cytoplasm but even in nuclei without any transfection agents or auxiliary procedures.

3. Conclusions

In this work we used the click chemistry to develop the delivery system for 2′-deoxyribonucleoside triphosphates. Our data confirmed the successfulness of the Huisgen's 1,3-dipolar cycloaddition reaction for the preparation of the SiO_2–dNTP nanocomposites. The fact that polymerase can recognize and incorporate nucleoside triphosphates in such nanobiocomposites into a growing DNA chain is of great importance. The results demonstrated a possibility of the utilization of SiO_2 nanoparticles as vehicles for the delivery of nucleoside triphosphates analogues into cells. It was shown that the proposed SiO_2–dNTP nanocomposites penetrated into eukaryotic cells and even in cellular nuclei. This makes it possible to use the nanobiocomposites bearing nucleoside triphosphate analogues as promising therapeutic drugs.

4. Experimental section

4.1. General

The following reagents were used: 2,2′-dithiodipyridine, fluorescein isothiocyanate isomer I, N-hydroxysuccinimide, butyl acetate, tris[(1-benzyl-1*H*-1,2,3-triazol-4-yl)methyl]amine (TBTA), copper(II) sulfate pentahydrate, and (+)-Sodium L-ascorbate crystalline (Sigma–Aldrich, USA); 6-bromohexanoic acid (Alfa Aesar);

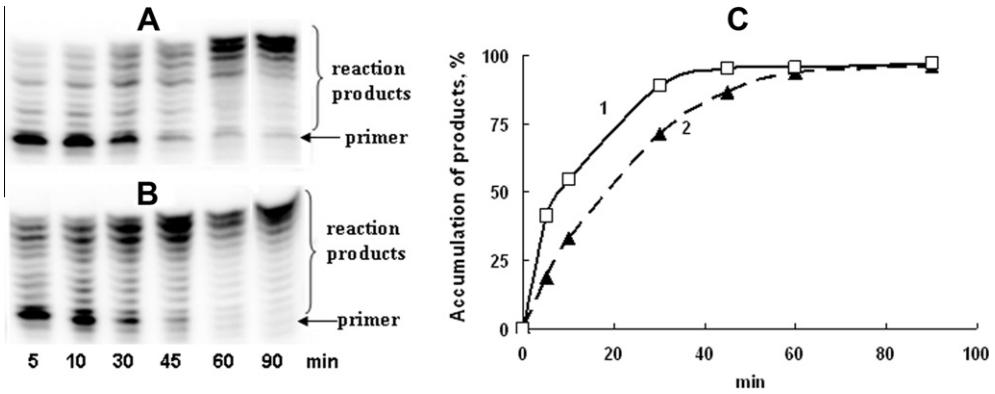

Figure 2. Electrophoresis in 20% PAAG of the extension products in the template (30-mer)/[^{32}P]primer (16-mer) system at 37 °C in the presence of Klenow fragment (5×10^{-3} U) and three native dNTP + SiO_2–dCTP (A) or four native dNTP (B) kinetic curves of these processes in the presence of four native dNTP (1) or three native dNTP + SiO_2–dCTP (2) concentrations: 4×10^{-6} M for the template, 1×10^{-6} M for the primer, 1×10^{-5} M for dNTPs; 0.07 mg/ml for SiO_2–dCTP (1×10^{-5} M for dCTP) (C).

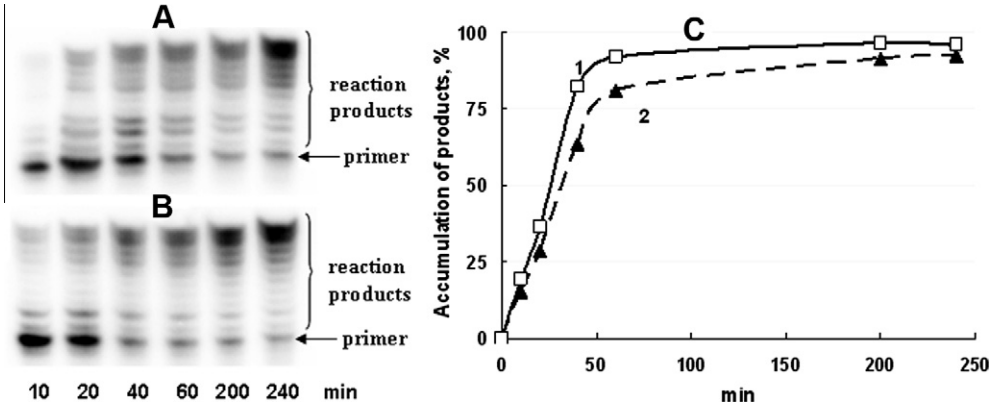

Figure 3. Electrophoresis in 20% PAAG of the extension products in the template (30-mer)/[^{32}P]primer (16-mer) system at 37 °C in the presence of HIV RT (2 U) and three native dNTP + SiO_2–dCTP (A) or four native dNTP (B) kinetic curves of these processes in the presence of four native dNTP (1) or three native dNTP + SiO_2–dCTP (2) concentrations: 4×10^{-6} M for the template, 1×10^{-6} M for the primer, 1×10^{-5} M for dNTPs; 0.07 mg/ml for SiO_2–dCTP (1×10^{-5} M for dCTP) (C).

triphenylphosphine (Fluka Chemie AG, Buchs, Switzerland); dicyclohexylcarbodiimide (Merck, Germany); SiO_2–NH_2 nanoparticles (SkySpring Nanomaterials, Inc., USA); deoxynucleoside triphosphates (ICBFM, Russia). 5-(3-Aminopropoxyprop-1-ynyl)-2′-deoxycytidin-5′-triphosphate, 3-propynyloxypropylamine, 2′-deoxycytidine-5′-triphosphate (trimbuthylammonium salt) and 1 M TEAAc buffer (pH 7) were acquired from 'NanoTech-S' LLC (Novosibirsk, Russia). All other reagents were from Sigma–Aldrich (Milwaukee, WI, USA). Organic solvents were dried and purified by standard procedures. ^{1}H and ^{31}P NMR spectra were recorded on Bruker AV-400 and AV-300 spectrometers.

The chemical shifts (δ) are reported in ppm relative to the residual solvent signals. In case of ^{31}P, an external standard of 85% H_3PO_4 was used. The coupling constant (J) values are expressed in Hertz (Hz) and spin multiples are given as s (singlet), d (doublet), t (triplet), q (quartet), m (multiplet), app.t (apparent triplet), and br (broad singlet). Matrix-assisted laser desorption/ionization-time of flight (MALDI-TOF) mass spectra were registered on a Reflex III spectrometer (Bruker Daltonics, Germany) in a positive detector mode with dihydroxybenzoic acid as a matrix. UV-absorption spectra were recorded on a UV-1800 spectrophotometer (Shimadzu, Japan). The presence of the azide functional group was registered by a Bruker Tensor 27 spectrometer (IR-spectra). SAXS patterns from the samples of sols of SiO_2–NH_2, SiO_2–dCTP, and SiO_2–dUTP(Flu) nanoparticles were measured on the small-angle X-ray diffractometer Kristalloflex-805 (Siemens, Germany). The product yields (Schemes 2 and 3) were evaluated as described in the figure legends. Aliquots of the reaction mixtures were taken off at the appropriate time, 10-fold diluted with water or ethanol, centrifuged, and analyzed by analytical anion exchange HPLC or analytical reverse phase HPLC. The analytical anion exchange chromatography was performed on a Milichrom-4 chromatograph (Econova, Russia) using a 2.5 × 60 mm column packed with Polysil SA, 15 μm (Vector, Russia). A linear gradient (flow rate 50 μL/min) from 0 to 0.8 M of K_2HPO_4/KH_2PO_4 (pH 7.0) was used. Preparative anion exchange chromatography was performed on DEAE Sephadex A-25, 40–120 μ, (Pharmacia Fine Chemicals, Sweden). Analytical reverse phase HPLC was performed using a Milichrom A-02 chromatograph (Econova, Russia) and a 2 × 75 mm column packed with ProntoSIL 120-5C18 AQ (Bischoff, Leonberg, Germany). Preparative reverse phase chromatography was performed on Polygoprep C18, 50–100 μ (Macherey-Nagel, Germany). Thin layer chromatography was carried out using Alufolien Kieselgel 60 F254 plates (Merck, Germany) in appropriate solvent mixtures and was visualized by UV irradiation, ninhydrin (for amine groups), or cystein/aqueous sulphuric acid (for nucleoside-containing compounds).

4.2. Synthesis of 6-azidohexanoic acid 1a

The synthesis of 6-azidohexanoic acid **1a** was carried out as described in[32] (Scheme 4B) from the corresponding bromoacid, DMSO was removed by evaporation with butyl acetate that increased the yield of the desired products by 20%. DMF can be also

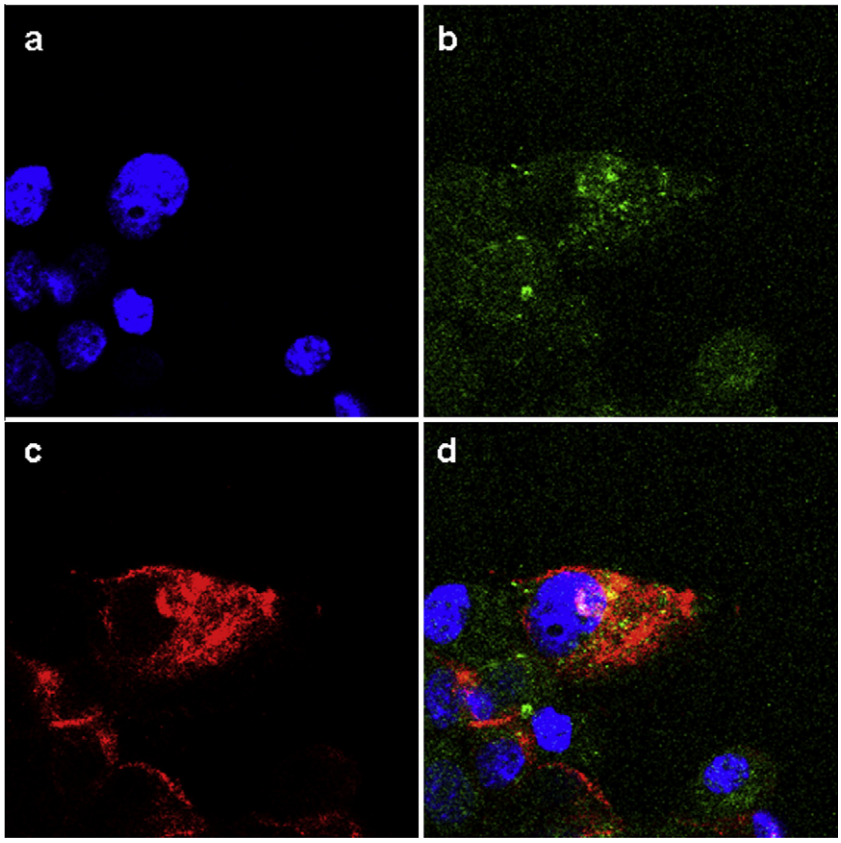

Figure 4. Confocal laser scanning microscope images of HeLa cells after incubation with SiO_2–dNTU^{Flu}. (a) nuclei stained with DAPI blue (405 nm); (b) fluorescein-labeled nanocomposites, green (488 nm); (c) cell membranes stained with Cell Mask Plasma Membrane Stain (543 nm), (d) superposition of channels (a–c).

used as a solvent. After the removal of residual solvent by evaporation at 56 °C, the yield of the final product **1a** was 78%. Spectral characteristics of the product correspond to those previously described.[32]

4.3. Synthesis of succinimidyl 6-azidohexanoate 1b (Scheme 4B)

6-Azidohexanoic acid (1.2 g, 7.64 mmol) was added to a solution of N-hydroxysuccinimide (966 mg, 8.4 mmol) in dichloromethane (10 mL). The dicyclohexylcarbodiimide solution (1.73 g, 8.4 mmol) in dichloromethane (4 mL) was then added, and the reaction mixture was left overnight at room temperature. Dicyclohexylurea was removed by filtration, and the filtrate was concentrated under reduced pressure to yield white crystals (1.84 g, 95% yield). Spectral characteristics of **1b**: ^{1}H NMR ($CDCl_3$, 400 MHz): δ ($CHCl_3$ = 7.26 ppm), 3.29 (t, 2H, CH_2N_3), 2.85 (dd, 4H, Suc), 2.63 (t, 2H, CH_2COOH), 1.77 (m, 2H, $N_3CH_2CH_2$), 1.63 (m, 2H, CH_2CH_2COOH), 1.51 (m, 2H, $N_3CH_2CH_2CH_2$); IR: N=N=N 2090 cm^{-1}.

4.4. Synthesis of azidomodified nanoparticles 1 (Scheme 4A)

SiO_2–NH_2 nanoparticles (2 mg, 0.5 μmol/mg for the amino groups) was suspended in 0.2 ml of a water/dimethylformamide mixture (1:1), followed by the addition of N-hydroxysuccinimide ester of 6-azidohexanoic acid (*N*-SEHA) (0.65, 2.5 or 10 mg, i.e., 2.5, 10, or 40-fold excess over the amino groups in nanoparticles). After stirring the mixture for 1 h at room temperature, it was centrifuged; supernatant was removed, and the particles were washed by acetone (3 × 0.1 ml) and ether (1 × 0.1 ml) and air-dried. IR spectra of the samples 1–3, respectively are presented in Supplementary data.

Synthesis of SiO_2–NH–CO–$(CH_2)_5$–N_3 for subsequent experiments was carried out using eightfold excess of *N*-SEHA over the amino groups in SiO_2–NH_2. 0.2 M *N*-SEHA (200 μl in dimethylformamide) was added to the SiO_2–NH_2 suspension (20 mg, 0.5 μmol/mg for the amino groups) in 0.6 ml of a water/dimethylformamide mixture (1:1) (the first addition). In 30-min intervals, the second and the third portions of *N*-SEHA (by 100 μl) were added to the reaction mixture. After stirring the mixture for 30 min at room temperature, it was centrifuged; supernatant was removed, and the particles were washed by acetone (3 × 1 ml) and ether (1 × 1 ml) and air-dried.

The amount of the amino groups before and after the treatment of SiO_2–NH_2 was evaluated by the picric acid method.[25] The yield of the reaction was evaluated to be 85%.

4.5. Synthesis of 2′-deoxycytidine-5′-{*N*-[3-(prop-1-ynyl)oxypropyl]-gamma-amino}-triphosphate 2

2,2′-Dithiodipyridine (198 mg, 0.9 mmol, 5 equiv) and triphenylphosphine (236 mg, 0.9 mmol, 5 equiv), in DMSO (150 μL each) were added to a solution of 2′-deoxycytidine-5′-triphosphate (tributhylammonium salt; 0.18 mmol) in DMSO (3 mL). After stirring the reaction mixture for 30 min, the solution of 3-propynyloxypropylamine[23] was added (200 μL, 1.8 mmol, 10 equiv), and the mixture was incubated at rt for 2 h. The resulting product was purified by anion exchange chromatography on DEAE Sephadex A-25. The elution was performed with a linear gradient from 20% EtOH to 1 M NH_4HCO_3 in 20% EtOH (150 mL each). Appropriate fractions were collected and evaporated. The residue was co-evap-

orated several times with aqueous ethanol to remove traces of the buffer. Target 2′-deoxycytidine-5′-{*N*-[3-(prop-1-ynyl)oxypropyl]-gamma-amino}-triphosphate **2** was precipitated by the addition of 6% $NaClO_4$ in acetone to the aqueous solutions of the product. The yield was 0.094 mmol (52%). ^{31}P (121.5, D_2O) δ: −0.83 (d, 1P, P_γ, *J* 20.9), −10.94 (d, 1P, P_α, *J* 20.9), −22.59 (t, 1P, P_β, *J* 18.6). ^1H (300, D_2O) δ: 8.0 (d, 1H, H(6), *J* 7.4); 6.36 (app.t, 1H, H1′, *J* 6.86); 6.32 (d, 1H, H(5), *J* 7.4); 4.61 (m, 1H, H4′); 4.18 (m, 5H, H3′, O–CH_2–C≡C, O–CH_2–CH_2–CH_2–NH); 3.64 (t, 2H, O–CH_2–CH_2–CH_2–NH, *J* 6.43); 3.00–2.93 (m, 2H, H5′); 2.47–2.27 (m, 2H, H5′); 1.80–1.76 (m, 2H, O–CH_2–CH_2–CH_2–NH). LC–MSD-Trap-XCT, $[M+H]^+$: calcd 579.09 $[M+H]^+$, found 579.08; calcd 601.09 $[M+Na]^+$, found 601.08; calcd 623.09 $[M+2Na]^+$, found 623.07; calcd 645.09 $[M+3Na]^+$, found 645.07.

4.6. Synthesis of 5-(3-aminopropoxyprop-1-ynyl)-2′-deoxyuridine-5′-{*N*-[3-(prop-1-ynyl)oxypropyl]-gamma-amino}-triphosphate 3a

2,2′-Dithiodipyridine (33 mg, 0.15 mmol), and triphenylphosphyne (39 mg, 0.15 mmol) in DMSO (50 μL each) were added to a solution of 5-(3-trifluoroacetamidopropoxyprop-1-ynyl)-2′-deoxyuridine-5′-triphosphate[23] (tributhylammonium salt; 0.031 mmol) in anhydrous DMSO (0.507 mL). After stirring the reaction mixture for 30 min, the 3-propynyloxypropylamine[23] solution was added (50 mg, 0.44 mmol), and the mixture was incubated at rt for 2 h. The resulting product was purified as in the case of compound **2** (see above). The protected 5′-triphosphate was subjected to the standard deprotection protocol (ammonia treatment for the trifluoroacetic protective groups). After the deprotection, resulting 5-(3-aminopropoxyprop-1-ynyl)-2′-deoxyuridine-5′-{*N*-[3-(prop-1-ynyl)oxypropyl]-gamma-amino}-triphos phate **3a** was precipitated by the addition of 6% $LiClO_4$ in acetone to the aqueous solution of the product. UV spectrum: (water), λ_{max}/nm (ε): 280 (14,400). According to the UV-spectral data, the yield was 0.020 mmol (64%). ^{31}P (121.5, D_2O) δ: −0.28 (d, 1P, P_γ, *J* 20.82), −10.66 (d, 1P, P_α, *J* 20.82), −21.28 (t, 1P, P_β, *J* 19.78). ^1H (300, D_2O) δ: 7.86 (m, 1H, H(6)); 6.16 (m, 1H, H1′); 4.42 (m, 1H, H4′); 4.27 (s, 2H, O–CH_2–C≡C–(L_1)); 3.98 (m, 5H, H5′, O–CH_2–C≡C–(L_2), H3′); 3.41 (m, 4H, O–CH_2–CH_2–CH_2–N (L_1), O–CH_2–CH_2–CH_2–N (L_2)); 2.92–2.75 (m, 4H, O–C_2–CH_2–CH_2–N (L_1), O–CH_2–CH_2–CH_2–N (L_2)); 2.16 (m, 2H, H2′); 1.74–1.60 (m, 4H, O–CH_2–CH_2–CH_2–N(L_1, L_2)).

4.7. Synthesis of 5-{3-[3-(fluorescein-5-yl-thioureido)propoxy]prop-1-ynyl}-2′-deoxyuridine-5′-{*N*-[3-(prop-1-ynyl)oxypropyl]-gamma-amino}-triphosphate 3

5-(3-Aminopropoxyprop-1-ynyl)-2′-deoxyuridine-5′-{*N*-[3-(prop-1-ynyl)oxypropyl]-gamma-amino}-triphosphate **3a** (10 mg, 0.014 mmol) was dissolved in 1 M carbonate–bicarbonate buffer, pH 9.0 (0.8 mL), followed by the addition of the fluorescein isothiocyanate solution (55 mg, 0.14 mmol) in a DMSO/DMF mixture (1:1, v/v, 0.40 mL). The reaction mixture was stirred for 2 h, the reaction products were then precipitated with 6% $LiClO_4$ in acetone (14 mL), centrifuged, and the precipitate was washed with acetone (3 mL) and ester. The target compound was purified by the reverse phase chromatography on Polygoprep C_{18} in a gradient of EtOH (0–10%) in water and precipitated with 6% $LiClO_4$ in acetone. R_f = 0.17 (Pr_iOH-conc. NH_3–H_2O, 7:1:2). The yield of **3** was 70%. ^{31}P (121.5, D_2O) δ: −0.39 (d, 1P, P_γ, *J* 20.35), −10.77 (d, 1P, P_α, *J* 20.35), −21.96 (t, 1P, P_β, *J* 20.35). ^1H (300, D_2O) δ: 7.80 (s, 1H, H(6)); 7.56 (m, 1H, Flu4); 7.50–7.47 (m, 1H, Flu6); 7.24–7.21 (m, 1H, Flu7); 7.01 (m, 2H, Flu4′,5′), 6.54–6.50 (m, 2H, Flu1′,3′), 6.39–6.33 (m, 2H, Flu7′,2′), 5.98 (m, 1H, H1′); 4.82 (m, 1H, H4′); 4.30 (s, 2H, O–CH_2–C≡C–(L_1)); 3.90 (m, 5H, H5′, O–CH_2-C≡C–(L_2), H3′); 3.66 (m, 4H, O–CH_2–CH_2–CH_2–N (L_1), O–CH_2–CH_2–CH_2–N (L_2)); 3.49 (m, 2H, O–CH_2–CH_2–CH_2–NH–Flu (L_1)); 2.82 (m, 2H, O–CH_2–CH_2–CH_2–N (L_2); 2.10 (m, 2H, H2′); 1.89 (m, 2H, O–CH_2–CH_2–CH_2–N(L_1)); 1.66 (m, 2H, O–CH_2–CH_2–CH_2–N(L_2)). LC–MSD-Trap-XCT, $[M+H]^+$: calcd 1063.81$[M+H]^+$; found 1063.4. calcd 1069.8 $[M+Li]^+$; found 1069.4.

4.8. Synthesis of SiO_2–dCTP 4 by 'click'-reaction (Scheme 1)

Azidomodified nanoparticles **1** (4 mg, 1.72 μmol) were suspended by sonication in 200 μL H_2O. Solution of 2′-deoxycytidine-5′-{*N*-[3-(prop-1-ynyl)oxypropyl]-gamma-amino}-triphosphate **2** (10 mM in H_2O, 344 μL, 3.44 μmol, 2 equiv) was added to the suspension followed by the addition of copper(II) sulfate pentahydrate (50 mM stock solution in H_2O, 44 μL), tris[(1-benzyl-1*H*-1,2,3-triazol-4-yl)methyl] amine (50 mM stock solution in DMSO, 44 μL), 1 M TEAAc buffer (pH 7, 20 μL), and sodium ascorbate (freshly prepared 0.1 M solution in water, 64 μL). The reaction mixture was degassed with argon for 2 min and stirred at room temperature for 24 h. The modified SiO_2-bound triphosphate was centrifuged, supernatant was removed. The modified nanoparticles were successively washed with aqueous 0.1 M NaCl, water, and diethyl ether, followed by air-drying. The yield of the click product was approximately evaluated by IR spectra to be more than 50%, (see IR **1** and **4** in Supplementary data). More precisely the yield of the attachment of triphosphate **2** to nanoparticles evaluated by measuring the optical density of the resulting product SiO_2–dCTP dissolved in 0.2 M NaOH. It was 58%. (UV spectrum: (0.2 M NaOH), λ_{max}/nm (ε): 260 (7400)). Another way to evaluate the efficiency of modification was to compare the amount of triphosphate **2** added to the particles and its amount in combined supernatants after the treatment and washing by optical density (UV spectrum:water, λ_{max}/nm (ε): 260 (7400). The extent of the attachment of triphosphate **2** evaluated by the ratio of $(I_0–I_s)/I_0 \cdot 100\%$ (I_0 and *Is* are the values of the optical density of **2** in the initial solution and in supernatant, respectively) was 55%.

4.9. Synthesis of SiO_2–$dUTP^{Flu}$ 5 by 'click'-reaction (Scheme 1)

Azidomodified nanoparticles **1** (2.5 mg, 1 μmol) were ultrasonically suspended in 100 μL H_2O. Solution of 5-{3-[3-(fluorescein-5-yl-thioureido)propoxy]prop-1-ynyl}-2′-deoxyuridine-5′-{*N*-[3-(prop-1-ynyl)oxypropyl]-gamma-amino}-triphosphate **3** (10 mM in H_2O, 543 μL, 5.043 μmol) was added to the suspension, followed by the addition of copper(II) sulfate pentahydrate (50 mM stock solution in DMSO, 22 μL), tris[(1-benzyl-1*H*-1,2,3-triazol-4-yl)methyl] amine (50 mM stock solution in DMSO, 22 μL), 1 M TEAAc buffer (pH 7, 15 μL), and sodium ascorbate (freshly prepared 0.1 M solution in water, 40 μL, 4 μmol). The reaction mixture was degassed with argon for 2 min and stirred at room temperature for 24 h.

The modified nanoparticles containing the bound fluorescent-labeled triphosphate was centrifuged, supernatant was removed. Modified nanoparticles were successively washed with aqueous 0.1 M NaCl, water, and diethyl ester, followed by air-drying. The yield of the click product evaluated by IR spectra was ~40%, see IR **1** and **5** in Supplementary data. The yield of the modification evaluated by optical density of the resulting product SiO_2–$dUTP^{Flu}$ **5** dissolved in 0.2 M NaOH. It was 50%. (UV spectrum: (0.2 M NaOH), λ_{max}/nm (ε): 280 (14,400)).

4.10. Synthesis of SiO_2–L–NH_2 6 by 'click'-reaction (Scheme 4C)

Azidomodified nanoparticles **1** (0.7 mg, 0.28 μmol) were suspended by sonication in 50 μL H_2O. 3-Propynyloxypropylamine (11 mg 0.1 mmol) was added to the suspension followed by the

addition of copper(II) sulfate pentahydrate (50 mM stock solution in DMSO, 22 μL), tris[(1-benzyl-1*H*-1,2,3-triazol-4-yl)methyl] amine (TBTA, 50 mM stock solution in DMSO, 22 μL), 1 M TEAAc buffer (pH 7, 10 μL), and sodium ascorbate (freshly prepared 0.1 M solution in water, 32 μL, 3.2 μmol). The reaction mixture was degassed with argon for 2 min and stirred at room temperature for 24 h. The modified nanoparticles containing the bound aminolinker (L) were centrifuged, and successively washed with aqueous 0.1 M NaCl, water, and diethyl ester, followed by air-drying. The yield of the 'click'-product was evaluated by IR spectra approximately100%, (see IR **6** in Supplementary data).

4.11. Primer extension reaction

Klenow fragment and 10× SE Klenow buffer containing 500 mM Tris–HCl, pH 7.6, 100 mM $MgCl_2$, and 50 mM DTT (Sibenzyme, Russia) or HIV RT and 10× RT buffer containing 500 mM Tris–HCl, pH 8.3, 750 mM KCl, 30 mM $MgCl_2$, and 50 mM DTT (Applied Biosystems, USA) were used in our experiments.

The mixture of the primer (16-mer, 10^{-4} M, 4 μL), the template (30-mer, 10^{-4} M, 4 μL), and 10× Klenow buffer (8 μL) was adjusted with water to 80 μL, kept at 95 °C for 5 min and cooled to room temperature for 30 min. The resulting duplex was used for the extension reactions.

The extension reaction was carried out in a mixture (20 μL) containing the above duplex (4 μL), Klenow buffer (2 μL), Klenow fragment (1×10^{-3} U), and 2 μL of each of dNTP (four native dNTPs (mixture 1), or three native dNTP except dCTP (mixture 2), or three native dNTP + SiO_2–dCTP (mixture 3), or three native dNTP + supernatant from SiO_2–dCTP suspension (mixture 4)). The final concentrations of the components in each reaction mixture were 4×10^{-6} M for the template, 1×10^{-6} M for the primer, 1×10^{-5} M for dNTPs; 0.07 mg/ml for SiO_2–dCTP (1×10^{-5} M for triphosphate in this nanocomposite). The reaction was carried out at 37 °C for 60 min 3 M $LiClO_4$ (30 μL) was added to each reaction mixture. In case of the presence of SiO_2–dCTP, reaction mixtures were centrifuged (14,000×*g*, 5 min) for separation of SiO_2 nanoparticles. The reaction products from each reaction mixture were precipitated with acetone (500 μL), centrifuged, washed with acetone, dried, dissolved in water (10 μL), and subjected to electrophoresis in 20% PAAG. After electrophoresis, the gel was stained with Stains All, dried in a FB GD 45 Gel dryer (Fisher Scientific, USA), and scanned (Fig. 1).

4.12. Kinetics of primer extension reaction

The primer/template duplex was prepared using the mixture of radioactive-labeled [^{32}P]primer (16-mer, 10^{-4} M, 4 μL), template (30-mer, 10^{-4} M, 4 μL), and Klenow buffer or HIV RT buffer (8 μL). The mixture was adjusted with water to 80 μL and kept at 95 °C for 5 min and cooled to room temperature for 30 min.

The reaction mixture containing 20 μL of the pre-formed duplex, 10 μL of corresponding 10× buffer (HIV RT or Klenow fragment), four native 10^{-4} M dNTPs (10 μL of each), and polymerase (5×10^{-3} U of Klenow fragment or 2 U of HIV RT) were adjusted with water to 100 μL. Concentration of SiO_2–dCTP added instead of dCTP was 0.7 mg/mL (10^{-4} M for dCTP). The final concentrations of the components in the reaction mixture (100 μL for each polymerase) were 4×10^{-6} M for the template, 1×10^{-6} M for the primer, 1×10^{-5} M for dNTPs; 0.07 mg/ml for SiO_2–dCTP (1×10^{-5} M for triphosphate in this nanocomposite). The reaction was carried out at 37 °C. Aliquots (10 μL) were taken from the reaction mixtures at regular intervals, followed by the addition of 3 M $LiClO_4$ (20 μL). In case of the presence of SiO_2–dCTP, reaction mixtures were centrifuged (14,000×*g*, 5 min) for separation of SiO_2 nanoparticles. The reaction products in all cases were precipitated with acetone (500 μL), centrifuged, washed with acetone, dried, dissolved in water (10 μL), and subjected to electrophoresis in 20% PAAG. After electrophoresis, the gel was dried in a FB GD 45 Gel dryer (Fisher Sscientific, USA) and scanned on a Molecular Imager FX-PRO Plus (Bio-Rad, USA). The reaction yields were evaluated using the Gel-Pro Analyzer 4.0 program (MediaCybernetics, United States) by determining the integral optical density (IOD) of spots in each lane (Figs. 2 and 3).

4.13. Penetration of SiO_2–$dUTP^{Flu}$ into HeLa cells

HeLa cells were cultured on glass cover slips (Invitrogen, USA) in RPMI media supplemented with 5% fetal calf serum (5%), penicillin and streptomycin (100 μg/ml, each) at 37 °C in a humidified incubator under ambient pressure air atmosphere containing 5% CO_2. At approximately 70% confluence, cells were treated with the SiO_2–$dUTP^{Flu}$ nanocomposite (2 nmol/ml) for 24 h and fixed with formaldehyde (3.7%) for 10 min, followed by washing with PBS. Nuclei and cell membranes were stained with DAPI and Cell Mask Plasma Membrane Stain (Molecular Probes, Invitrogen, USA), respectively for 10 min. After washing the cells with PBS, they were visualized by confocal laser scanning LSM 510 UV META microscope (Carl Zeiss, Inc., Germany). Laser lines were 405 nm (for nuclei, DAPI blue), 488 nm (for fluorescein-labeled nanocomposites, green), and 543 nm (for cell membranes, red) (Fig. 4).

Acknowledgments

Authors thank S. I. Baiborodin for the assistance in the use of confocal fluorescent microscopy and F. V. Tuzikov for the assistance in the analysis of the size of nanoparticles. The work was supported by RFBR Grant no. 11-04-01408-a.

Supplementary data

Supplementary data associated with this article can be found, in the online version, at http://dx.doi.org/10.1016/j.bmc.2012.11.057.

References and notes

1. Vivet-Boudou, V.; Didierjean, J.; Isel, C.; Marquet, R. *Cell. Mol. Life Sci.* **2006**, 163.
2. De Clercq, E.; Neyts, J. *Rev. Med. Virol.* **2004**, *14*, 289.
3. Hofheinz, R. D.; Gnad-Vogt, S. U.; Beyer, U.; Hochhaus, A. *Anticancer Drugs* **2005**, *16*, 691.
4. Lee, R. J. *Mol. Cancer Ther.* **2006**, *5*, 1639.
5. Vinogradov, S. V. *Expert Opin. Drug Deliv.* **2007**, *4*, 5.
6. Tiera, M. J.; Winnik, F. O.; Fernandes, J. C. *Curr. Gene Ther.* **2006**, *6*, 59.
7. Neu, M.; Fischer, D.; Kissel, T. *J. Gen. Med.* **2005**, *7*, 992.
8. Zhang, Z. Y.; Smith, B. D. *Bioconjug. Chem.* **2000**, *11*, 805.
9. Bashford, C. L.; Alder, G. M.; Menestrina, G.; Micklem, K. J.; Murphy, J. J.; Pasternak, C. A. *J. Biol. Chem.* **1986**, *261*, 9300.
10. Mislick, K. A.; Baldeschwieler, J. D. *Proc. Natl. Acad. Sci. U.S.A.* **1996**, *93*, 12349.
11. Morris-Natschke, S. L.; Ishaq, K. S.; Kucera, L. S. *Curr. Pharm. Des.* **2003**, *9*, 1441.
12. Langer, R.; Tirrell, D. A. *Nature (London)* **2004**, *428*, 487.
13. Hughes, G. A. *Nanomedicine* **2005**, *1*, 22.
14. Paunesku, T.; Rajh, T.; Wiederrecht, G.; Maser, J.; Vogt, S.; Stojicevic, N.; Protic, M.; Lai, B.; Oryhon, J.; Thurnauer, M.; Woloschak, G. *Nat. Mater.* **2003**, *2*, 343.
15. Park, J. H.; Gu, L.; Maltzahn, G.; Ruoslahti, E.; Bhatia, S. N.; Sailor, M. J. *Nat. Mater.* **2009**, *8*, 331.
16. Chen, M.; Mikecz, A. *Exp. Cell Res.* **2005**, *305*, 51.
17. Neumeyer, A.; Bukowski, M.; Veith, M.; Lehr, K. M.; Daum, N. *Nanomedicine* **2011**, *7*, 410.
18. Canham, L. T. *Adv. Mater.* **1995**, *1033*, 7.
19. Kolb, H. C.; Finn, M. G.; Sharpless, K. B. *Angew. Chem., Int. Ed.* **2004**, *2001*, 40.
20. Alvarez, R.; VelAzquez, S.; San-Felix, A.; Aquaro, S.; DeClercq, E.; Perno, C. F.; Karlsson, A.; Balzarini, J.; Camarasa, M. J. *J. Med. Chem.* **1994**, *37*, 4185.
21. Alagarsamy, V.; Meena, S.; Ramaseshu, K. V.; Solomon, V. R.; Kumar, T. *Chem. Biol. Drug Des.* **2007**, *70*, 158.
22. Aufort, M.; Herscovici, J.; Bouhours, P.; Moreau, N.; Girard, C. *Bioorg. Med. Chem. Lett.* **2008**, *18*, 1195.
23. Vasilyeva, S. V.; Budilkin, B. I.; Konevetz, D. A.; Silnikov, V. N. Nucleosides *Nucleotides Nucleic Acids* **2011**, *30*, 753.

24. Babkina, G. N.; Zarytova, V. F.; Knorre, D. G. *Bioorg. Khim.* **1975**, *1*, 611.
25. Atherton, E.; Sheppard, R. C.; Ward, P. *J. Chem. Soc., Perkin Trans. 1* **1985**, *10*, 2065.
26. Lee, L. A.; Mitchell, M. L.; Huang, S. J.; Fokin, V. V.; Sharpless, K. B.; Wong, C. H. *J. Am. Chem. Soc.* **2003**, *125*, 9588.
27. Perez-Balderas, F.; Ortega-Munoz, M.; Morales-Sanfrutos, J.; Hernandez-Mateo, F.; Calvo-Flores, F. G.; Calvo-Asin, J. A.; Isac-Garcia, J.; Santoyo-Gonzalez, F. *Org. Lett.* **1951**, *2003*, 5.
28. Seo, T. S.; Li, Z.; Ruparel, H.; Ju, J. *J. Org. Chem.* **2002**, *68*, 609.
29. Parrish, B.; Breitenkamp, R. B.; Emrick, T. *J. Am. Chem. Soc.* **2005**, *127*, 7404.
30. Tuzikov, F. V.; Zinoviev, V. V.; Vavilin, V. I.; Malygin, E. G. *Biopolymers* **1996**, *38*, 131.
31. Tuzikov, F. V.; Tuzikova, N. A.; Galimov, R. V.; Panin, L. E.; Nevinsky, G. A. *Med. Sci. Monit.* **2002**, *6*, 79.
32. Parrish, B.; Emrick, T. *Bioconjug. Chem.* **2007**, *18*, 263.